Int.J.Curr.Microbiol.App.Sci (2015) 4(1): 270-283

International Journal of Current Microbiology and Applied Sciences
ISSN: 2319-7706 **Volume 4 Number 1 (2015) pp. 270-283**
http://www.ijcmas.com

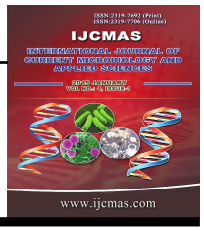

Original Research Article

Quantitative identification of phosphate using X-Ray diffraction and Fourier transform infra red (FTIR) spectroscopy

Mohammed Y. Eisa*, Motaz Al Dabbas and Fatma H. Abdulla

Central Environmental Laboratory-College of Science, University of Baghdad, Baghdad, Iraq
**Corresponding author*

Keywords

Iraqi Akashat phosphate ore, Calcareous phosphate, Quantitative identification, XDR, FTIR

A B S T R A C T

In this study, Fourier Transform Infrared Spectrophotometry (FTIR), X Ray Diffraction (XRD) and loss on ignition (LOI), comparatively employed to provide a quick, relatively inexpensive and efficient method for identifying and quantifying calcite content of phosphate ore samples taken from Akashat site in Iraq. A comprehensive spectroscopic study of phosphate-calcite system was reported first in the Mid-IR spectra (400–4000 cm^{-1}) using Shimadzu IR Affinity-1, for different cuts of phosphate field grades with samples beneficiated using calcination and leaching with organic acid at different temperatures. Then using the resulted spectra to create a calibration curve relates material concentrations to the intensity (peaks) of FTIR absorbance and applies this calibration to specify phosphate-calcite content in Iraqi calcareous phosphate ore. Their peaks were assigned to the fundamental vibration modes of PO_4^{-3} in phosphate and CO_3^{-2} in calcite. Thus FTIR appears to provide a fast and reliable method for identifying calcite concentrations in phosphate ore.

Introduction

Most commercial applications of phosphorus-containing materials are based on phosphoric acid and phosphate salts. A multitude of applications exist, including use in detergents, animal feed supplements, dentifrices, fertilizers, metal treating, water softening, leavening agents and fire retardants. On a weight bases, fertilizers remain the main single largest application (Kirk-Othmer, 1998).

Phosphate rocks are the main source of phosphate in the world. They are vital non-renewable resources and essential components in fertilizers and phosphorous based chemicals. It is neither substitutable nor recyclable, therefore, the total demand must be provided through the mining, beneficiation and chemical processing of natural resources of this ore. Phosphate deposits may be divided to three major groups, according to their origin:

1- Deposits from sea sediments.
2- Igneous and metamorphic deposits.
3- Biogenetic deposits.

It should be mentioned that most of world's phosphate resources are of sedimentary deposit origin (Al-Fariss *et al.,* 1992; Guimarães *et al.,* 2005).

According to (Becker, 1983) about 200 known minerals contain more than 1% P_2O_5. The most important minerals for the phosphoric acid industry are those belonging to the apatite group. The phosphate rock normally not only contains the apatite mineral, but also several other minerals, such as calcite, dolomite, pyrite, kaolinite, quartz, feldspar and fluorite (Gremillion and McClellan, 1975).

Apatite (the desired component in phosphate rock) has the general formula, $Ca_{10}(PO_4)_6X_2$ where X is typically F (fluorapatite, FAp), OH (hydroxyapatite, OHAp), or Cl (chlorapatite, ClAp). The apatite lattice is very tolerant of substitutions. The extent, to which substitution takes place and what the substitutes are, depends on the prevailing conditions when the apatite was formed and on the influence of subsequent events, such as weathering (Elliott, 1994).

Phosphate deposits in Iraq are of sedimentary origin. Its formations lie in the western border regions. The most important of these formations is Akashat phosphate layer in which the proportion of phosphorus pent-oxide between 21–22%. Phosphate deposits in sedimentary layers appears freely with limestone and clay stone (Shirqi and Tawfiq, 2010).

More than 80% of the world's raw phosphate came from sedimentary deposits. The raw phosphate contains several other minerals next to the apatite mineral. Only the apatite mineral is needed for the production of phosphoric acid. The raw phosphate is normally first washed with water to remove the water soluble minerals. Thereafter several steps are applied to remove the larger part of the other minerals and to obtain the phosphate ore. This process to obtain phosphate ore from raw phosphate is often called beneficiation. Carbonate gangue removal is a prerequisite prior to the digestion of the phosphate rock by an inorganic acid. Otherwise the development of carbon dioxide from the rock gives rise to excessive foaming (Van Der Sluis, 1987). In a previous work a new approach is developed to remove Dolomitic gangue material from phosphate ore using organic acids (Cicil *et al.,* 2014). In order to specify the optimum conditions of phosphate extraction which give minimum Dolomitic content, spectrometric methods used to identify beneficiated samples.

X-Ray Diffraction

X-ray diffraction (XRD) spectrometry is one of the most powerful analytical tools available for identifying unknown crystalline substances. All crystals are composed of regular, repeating planes of atoms that form a lattice. When coherent X-rays are directed at a crystal, some of them are scattered and the other are diffracted. These diffracted X-rays, which can be thought of as waves traveling in all directions, form interference patterns, much like interference patterns formed by dropping two rocks into water. This interference may be constructive, forming larger waves, or destructive, canceling out the waves entirely. The pattern of interference created depends on the distance between atomic layers, chemical composition, and the angle that the X-rays diffract away from the atoms, thus it indirectly reveals a crystals structure (Jenkins and Snyder, 1996).

Using an XRD spectrometer, the diffraction pattern created by constructive interference

is recorded by a beam detector as the X-ray tube and the detector are rotated around the sample. The relationship between angle at which diffraction peaks occur 2θ and the inter-atomic spacing of a crystalline lattice (d-spacing) is expressed in Equation 1 by Bragg's law:

$$n\lambda = 2d \sin\theta \quad \ldots \quad (1)$$

For historical reasons, XRD diffractograms are expressed in degrees two theta (2θ) (Bergslien *et al.,* 2008).

Since each crystalline structure is unique, the angles of constructive interference form a unique pattern. By comparing the positions and intensities of the diffraction peaks against a library of known crystalline materials, samples of unknown composition can be identified. This works even with mixtures of materials, where each separate crystalline material can be identified and semi quantified (Dinnebier *et al.,* 2008).

As the concentration of a phase in a mixture varies, the intensities of all of the peaks from this phase vary in concert (ideally). Thus, the concentrations of phases in a mixture can be determined by measuring the intensities of peaks in the powder pattern (Pecharsky and Zavalij, 2009; Clearfie *et al.,* 2008).

Apatite can be identified by a highest intensity peak located at approximately (2θ) 31.9^o, closely followed by three more high intensity peaks located between (2θ) 32^o and 34^o. Apatite also has weaker intensity diagnostic peaks located at approximately (2θ) 26^o as shown in Figure 1 (Tas, 2007).

The locations and intensities of these peaks clearly differentiate apatite from the vast majority of materials that are for the most part composed of calcium carbonates, silicates, or sulfates. For example, plaster of Paris (Gypsum), charcoal ash, wood ash and both kinds of sheetrock all lack peaks near (2θ) 11^o, calcite lack peak near (2θ) 29.4^o. If a sample lacks any of the diagnostic peaks listed and/ or the relative peak heights are significantly different, then the sample is not apatite, or the sample is contaminated (Bergslien *et al.,* 2008).

In the calcareous type phosphate ore, Dolomitic material (especially calcite) is the main constituent, so, its XRD pattern must be exactly recognized. Calcite can be characterized by a main peak near 2θ 29.5^o as shown in Figure 2 (Rungsarit *et al.,* 2012).

Foureir Transform Infra Red Spectroscopy (FTIR)

Fourier Transform Infrared Spectro-photometry (FTIR) spectra of minerals display characteristic features, usually absorption features, which can be related qualitatively to variations in the constituent minerals. Absorption features result from the detection of vibration modes, i.e. lattice vibrations and/or molecular group vibration modes. Qualitative mineral identification is possible because minerals have characteristic absorption bands in the midrange of the infrared, wave numbers 4000 to 400 cm^{-1}. Quantitative analysis with an FTIR is also possible because in simple two component mixtures, absorbance feature sizes are proportional to the concentration of each component as given by Beer's Law (Griffiths, 1986; Smith, 1995). Thus, to distinguish the presence of a specific group (bond) and also the degree of probable separation of a reacted component during acid treatment, FTIR analysis was performed in the present investigation.

A recent study (Ratner *et al.*, 2004) referred to the most characteristic chemical groups of the FTIR spectrum of hydroxyapatite are PO_4^{-3}, CO_3^{-2}, OH^{-1} and HPO_4^{-2}, as shown in Figure 3. Its absorbance spectrum is taken in the mid range of wave number (400–4000 cm^{-1}). In this figure, the stretching band at 3571 cm^{-1} and libration band at 634 cm^{-1} originate from OH^{-1} groups. The bands located at 474, 570, 603, 962, 1049, and 1089 cm^{-1} originate by PO_4^{-3} ions. The intensity of the O-H stretching vibration in hydroxyapatite is weaker than the strong P-O stretching vibration due to hydroxyapatite stoichiomety in both synthetic and natural hydroxyapatite (Markovic *et al.*, 2004).

However, the spectrum of a natural sample contains many components; it is significantly more difficult to extract the quantitative results. Though still based on Beer's law, the absorbance at a specific wavelength is the sum of the absorbance of all sample components that absorb at that wavelength.

Loss on Ignition (LOI)

It is the decrease in weight of the sample after being ignited from 550 to 950 °C. It refers to the amount of CO_2 in the sample. Dolomitic materials in the ore subjected to calcination according to the reactions (Abouzeid, 2008):

$$CaCO_3.MgCO_3 \longrightarrow CaO + MgO + 2CO_2$$

In the present work, loss on ignition test will be used to quantitatively identify Dolomitic materials (especially calcite) content to support the X-ray diffraction and FTIR spectral analysis.

Experimental Work

In order to identify the behavior of the phosphate bearing minerals and the associated impurities, representative samples of Akashat phosphate ore (crushed to -10 mm particle size) was subjected to dry sieving in the previous work. Using Standard Sieves, various size fractions of the sample were collected for analysis. The fraction of each particle was separated, weighed and percentage of each weight fraction was calculated as shown in Table 1 (Cicil *et al.*, 2014). The analysis was also carried out regarding average size, mass fractions and cumulative mass fraction.

All of the samples were dried in an electric oven at about 105°C for 2 hrs, cooled to room temperature and stored in closed desiccators. Each size fraction obtained was weighed and analyzed in terms of apatite and calcite. The distribution percentages were calculated accordingly.

These sample fractions were characterized by X-ray powder diffraction (Model Lab-X, XRD 6000, Shimadzu, Japan) in the National Center for Construction Laboratories and Research, Ministry of Construction and Housing.

Samples for XRD analyses were first ground in an agate mortar using an agate pestle and then sprinkled onto ethanol-damped single-crystal quartz sample holders to form a thin layer, followed by tapping to remove excess powder. The XRD was operated at 40 kV and 30 mA with monochromated Cu Ka radiation. XRD data over the range of angle (2θ=20–50o) were collected with a step size of 0.05 degree and a preset time of 0.75 sec at each step (Rungsarit *et al.*, 2012).

For FTIR analysis, 0.01 g of each sample mixture were mixed with 0.5 gm of spectral grade KBr, and finely ground in an agate mortar to nearly 40 μm size, thoroughly dried at 105°C, and pressed into pellets under about 10 tons/cm^2 pressure. Spectral

measurements were carried out on an FTIR spectrophotometer (Shimadzu, IR Affinity-1) that was operated in the absorbance mode, in the Central Environmental Laboratory, College of Science-University of Baghdad. Spectra were normally acquired with the use of 4 cm^{-1} resolution yielding IR traces over the range of 400–4000 cm^{-1}. All data were corrected for background spectrum. The sample chamber of the FTIR was kept desiccated, but was not evacuated and the background was corrected to remove the effect of any remaining H_2O. Each analysis takes about 30 sec; most of that time is spent gathering 22 spectra that are co-added to reduce noise. Theoretically noise should be reduced as the number of co-added spectra increases. However, our experiments showed a practical limit to this noise reduction with co-added spectra. Data were recorded as percent reflectance relative to KBr, which was used as a standard to calibrate the machine as many studies on FTIR (Herbert et. al., 1992; Featherstone *et al.*, 1984) and then record diffuse reflectance rather than absorbance.

Loss on ignition test (LOI) is then used to specify calcite content as it represented by the decrease in weight of the sample after being ignited from 550 to 950°C using Electrical furnace with controller unit board for time (min.) and temperature maximum 1300°C (NABERTHERM-N20/H-West Germany).

Results and Discussion

The FTIR spectrum of pure analytical grade calcium carbonate shown in Figure 4 express the presence of a strong band centered around 1425.4 cm^{-1}, characteristics of the C–O stretching mode of carbonate together with a narrow band around 875.68 cm^{-1} of the bending mode.

In the present work, among those bands described, the strong absorption bands of carbonate around 1425 cm^{-1} and the band centered around 1040 cm^{-1} of phosphate was used as analyte peaks for the analysis of the related components. The FTIR spectrum of the mixture of these two components showed that there is no significant interference to any of the analyte peak of a component from the other two components present in the matrix, thus the analyte peaks chosen, can be safely used for analysis of the individual components in their mixtures.

According to the collected data, quantification of the mixtures using FTIR absorption peaks supported with XRD patterns and Loss on ignition (LOI) tests, were employed to create a calibration curve that can be further used to predict the composition of phosphate ore samples based on their absorbance peak height data.

Figure 5 shows the FTIR spectra of the Akashat ore of sieve cut greater than 600 μm. It is clearly found from this figure that there are two main bands as discussed. The strong band centered around 1055.11 cm^{-1} which splits into components at the range 1037.75–1093.69 cm^{-1} and the small peaks at 472.58, 569.99 and 605.67 cm^{-1} are assigned to the stretching and bending modes respectively of phosphate in the apatite spectrum. The presence of a strong band centered around 1412.92 cm^{-1}, which splits into components at the range 1396.52-1428.35 cm^{-1} are characteristics of the CO_3^{-2} stretching mode of carbonate together with a narrow band around 873.79 cm^{-1} of the bending mode characteristic to the carbonate of calcite in the ore.

Intensity of absorbance data of Figure 5 demonstrates that two main components are dominant, hydroxyapatite and calcite. X ray diffraction (XRD) test of the same sample

enhances that result as shown in Figure 6. Two main peaks, one at (2θ) 31.9° closely followed by three more high intensity peaks located between (2θ) 32°-34° belong to apatite group. Another distinct main peak at (2θ) 29.4° belong to calcite which is the main constituent in the phosphate ore. Loss on ignition (LOI) test of this cut quantitatively confirms carbonate content in the phosphate cut sample. It was determined that loss on ignition for this cut was (25.87%) i.e. calcite content was (58.79%) by weight.

In the same way, the three tests were accomplished to the remaining cuts in addition to the beneficiated sample using lactic acid. In Figures 7–11, the FTIR spectra are shown for the mentioned samples, and then Figures 12–16 give the X ray diffractograms of the same samples. Data of loss on ignition tests are tabulated in Table 2 with the percentages relative intensity ratio results (RIR%) of the components based on the main intensities according to the relation given by (Raynaud *et al.*, 2001):

$$RIR = \frac{Intensity\ of\ major\ line\ of\ phase}{\sum Intensity\ of\ major\ lines\ of\ all\ phases}$$

In order to specify the relation between calcite content based on loss on ignition test with the X-ray diffraction and FTIR relative intensity ratio (RIR%) of calcite, data of Table 2 are plotted as given in Figure 17. It is clearly found from this Figure that there is large compatibility between the XRD and FTIR tests with the quantitative analysis of calcite content using loss on ignition test. To explain this compatibility more obviously, a regression analysis was achieved relating each of the two tests (XRD and FTIR) with the quantitative analysis data LOI and plot them as shown in Figure 18 using STATISTICA® release10. The regression gives equations represent the calcite content depending on the relative intensity ratio (RIR%) data as shown:

$Y=13.444+0.184*R_x+0.0054*R_x^2$
$R=0.99088$
$Y=-39.1828+3.5548*R_f-0.0323*R_f^2$
$R=0.9998$

Where:

Y = calcite content%, R_x = XRD relative intensity ratio%, R_f = FTIR relative intensity ratio%, R=correlation coefficient

Correlation coefficient values of the two relations are convergent to unity which ensures high prediction of calcite content based on XRD and FTIR spectral analysis.

A new quantitative chemical analysis method was developed to accurately determine the compositions of calcareous phosphate ore which contain calcite ($CaCO_3$) as a main constituent, and apatite [$Ca_{10}(PO_4)_6(OH)_2$] using FTIR and XRD main peak height measurements. Data collected from the study were used to create calibration curves for prediction of the ore components weight percentages. Testing results showed that these curves were successfully created and could be used to predict ore compositions.

Any impurity that does not influence the measured peak intensities is not expected to affect the calibration. Provided that the concentrations of impurities are determined by other analytical techniques, the calibration results obtained in this study can always be normalized through multiplication by (100-%impurities)/100.

Table.1 Particle size distribution of Akashat phosphate sample (Cicil *et al.*, 2014)

Fraction (mm)	Weight %
+0.60	29.13
+0.30	13.01
+0.15	20.05
+0.125	11.99
+0.075	13.05
-0.075 (base)	12.77

Table.2 Analysis results of Akashat phosphate ore based on loss on ignition, FTIR and X ray diffraction

No.	Size micron	LOI	% Calcite	XRD RIR%	FTIR RIR%
1	+600	25.87	58.7954	75.99	54.097
2	+300	22.746	51.6954	65.794	40.454
3	+250	21.67	49.25	65.23	37.779
4	+150	18.39	41.79545	61.313	32.097
5	+75	22.628	51.42727	67.562	40.28
6	-75	24.961	56.72955	75.507	48.143
7	Extracted Sample	7.618	17.3136	14.49	19.3

Figure.1 Typical XRD spectrum of Hydroxyapatite

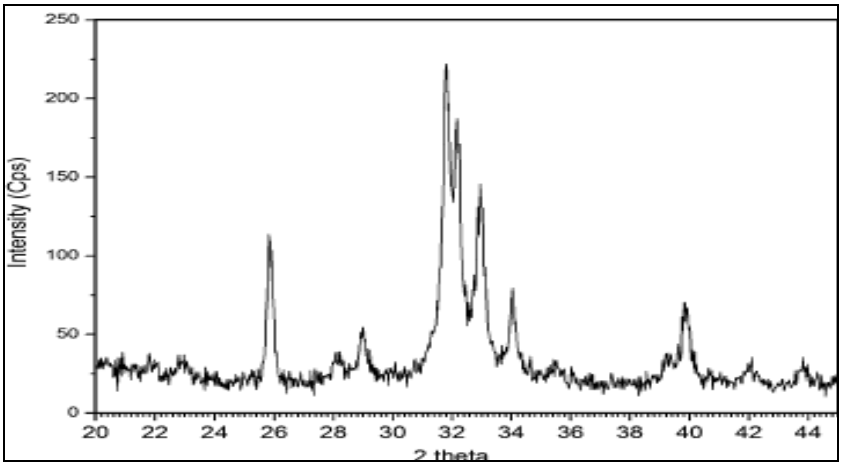

Figure.2 XRD pattern of $CaCO_3$ (Rungsarit *et al.*, 2012)

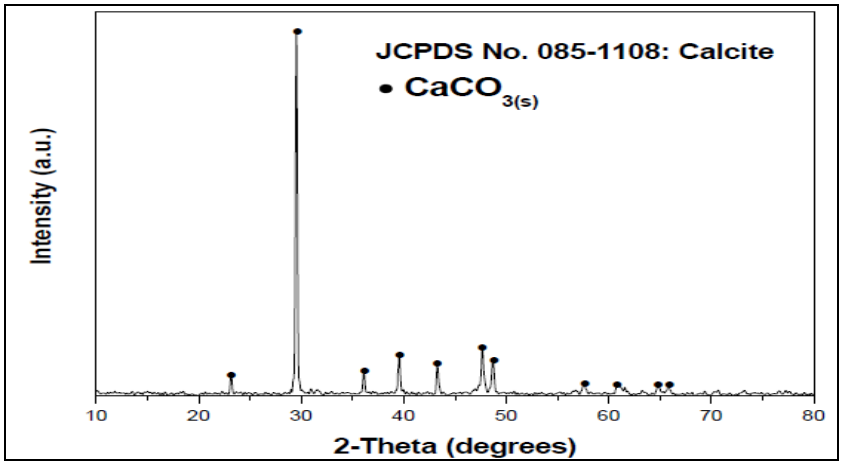

Figure.3 A typical FTIR spectrum of Hydroxyapatite

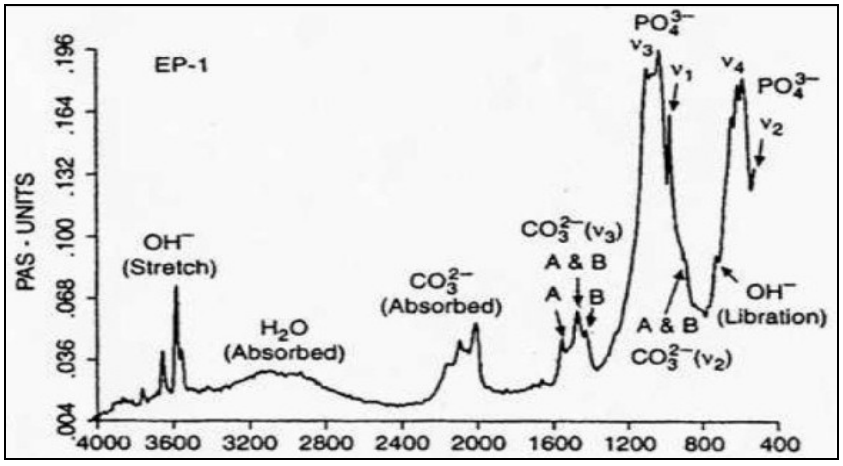

Figure.4 FTIR Spectrum of pure analytical grade calcite

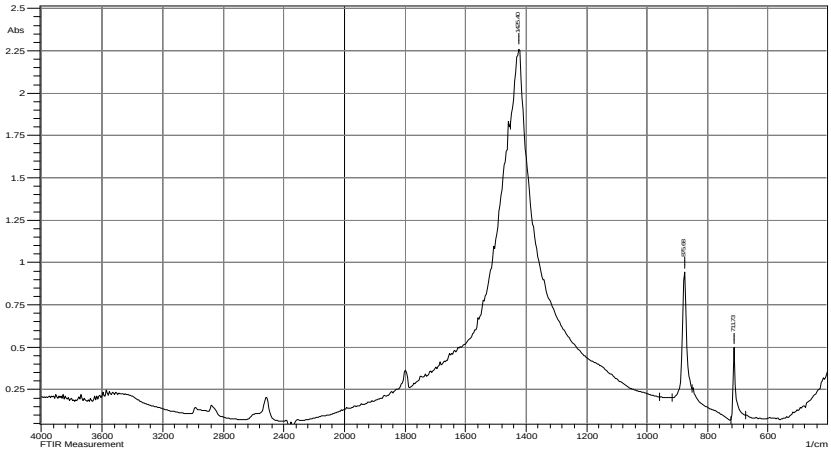

Figure.5 FTIR Spectra of +600 micron cut, Akashat phosphate Ore

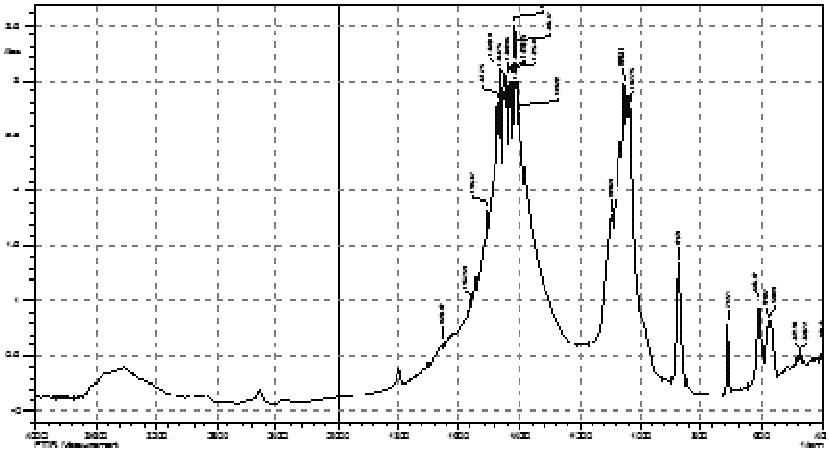

Figure.6 XRD Spectra of +600 micron cut, Akashat phosphate Ore

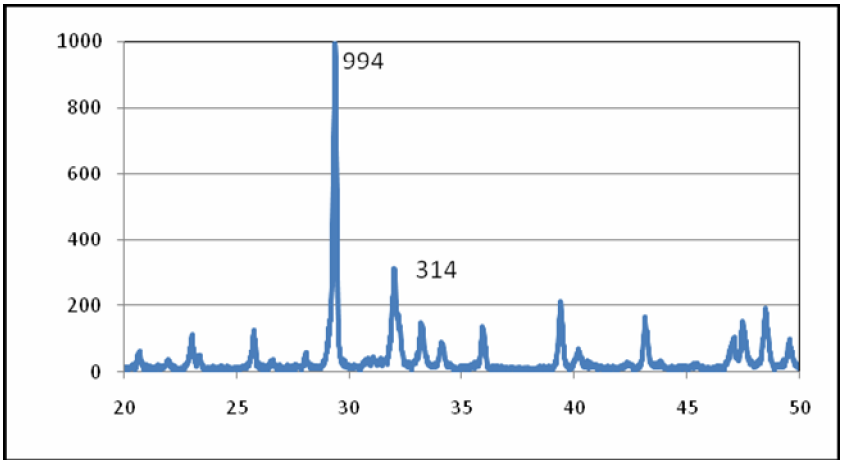

Figure.7 FTIR Spectra of +300 micron cut, Akashat phosphate Ore

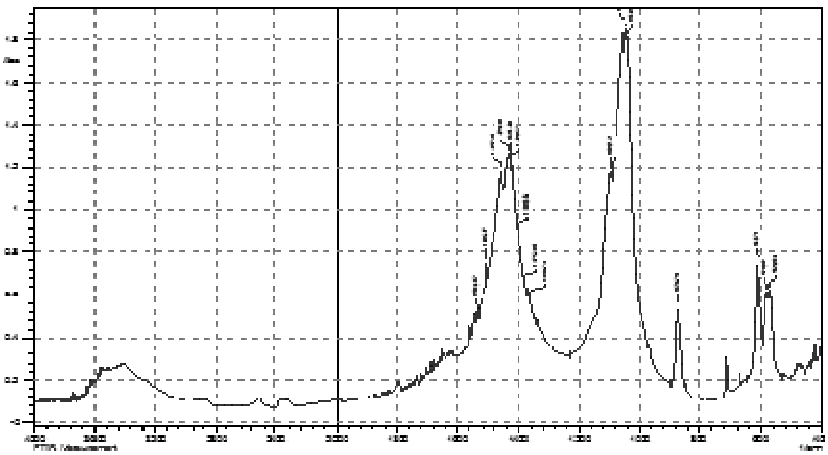

Figure.8 FTIR Spectra of +150 micron cut, Akashat phosphate Ore

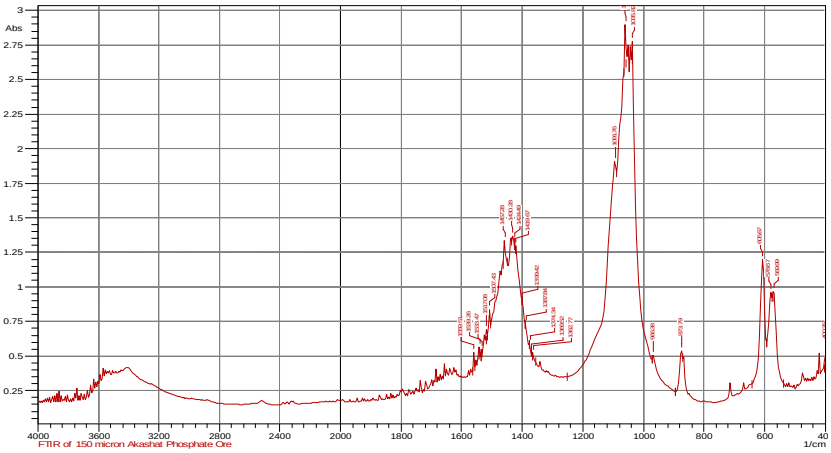

Figure.9 FTIR Spectra of +75 micron cut, Akashat phosphate Ore

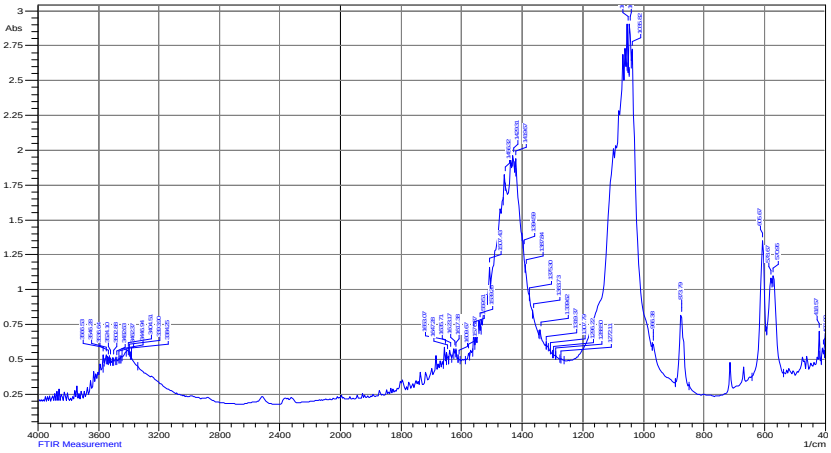

Figure.10 FTIR Spectra of -75 micron cut, Akashat phosphate Ore

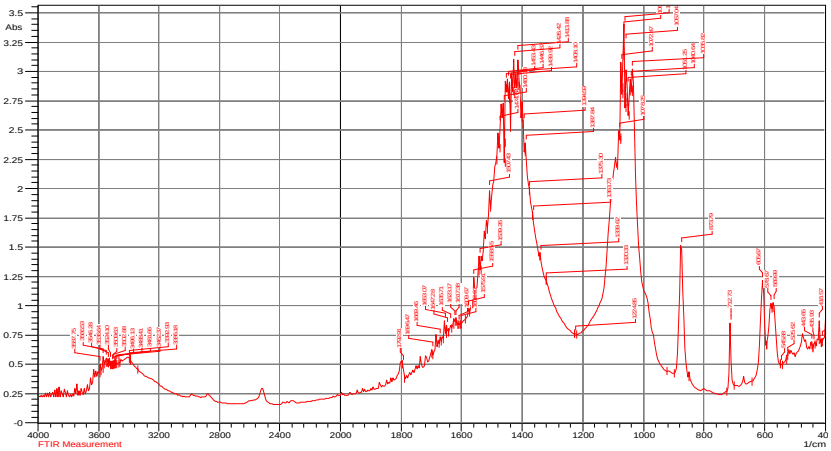

Figure.11 FTIR spectra of beneficiated Akashat phosphate ore using lactic acid

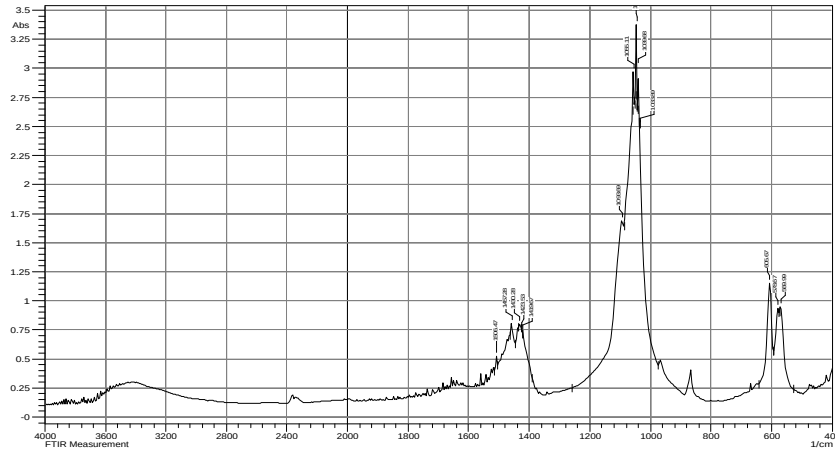

Figure.12 XRD spectra of +300 micron cut, Akashat phosphate ore

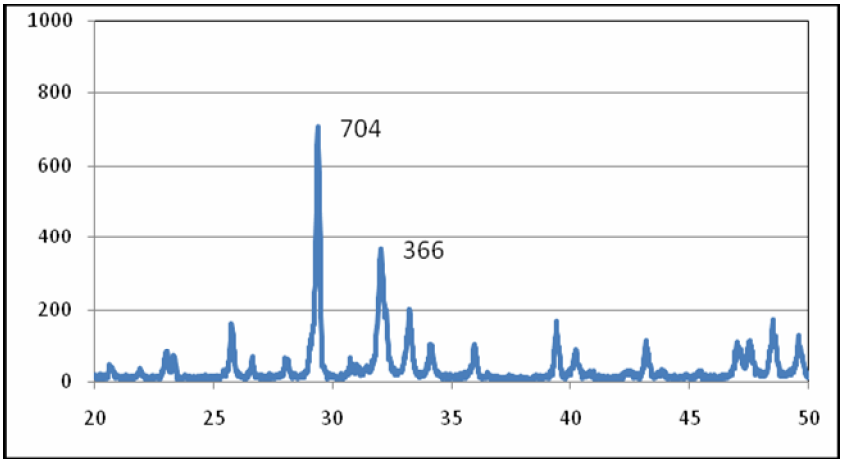

Figure.13 XRD Spectra of +150 micron cut, Akashat phosphate ore

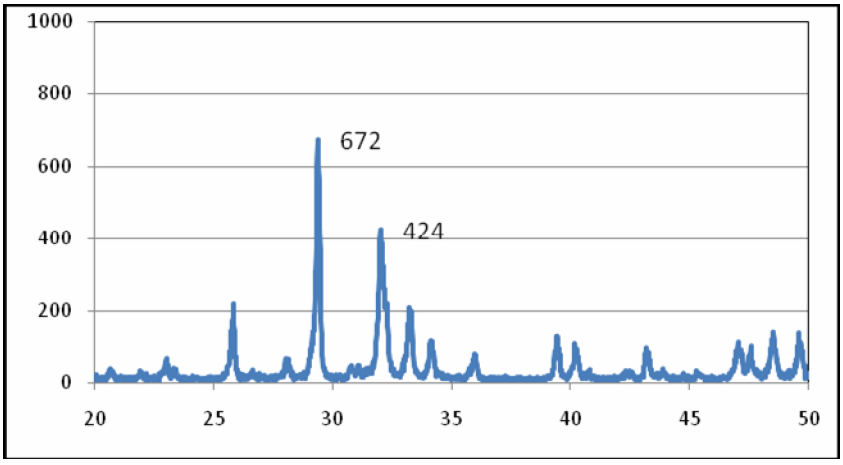

Figure.14 XRD Spectra of +75 micron cut, Akashat phosphate ore

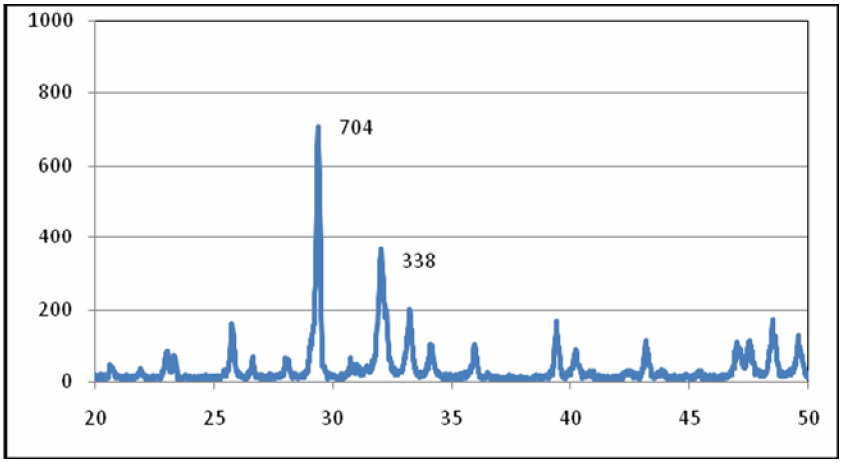

Figure.15 XRD Spectra of -75 micron cut, Akashat phosphate ore

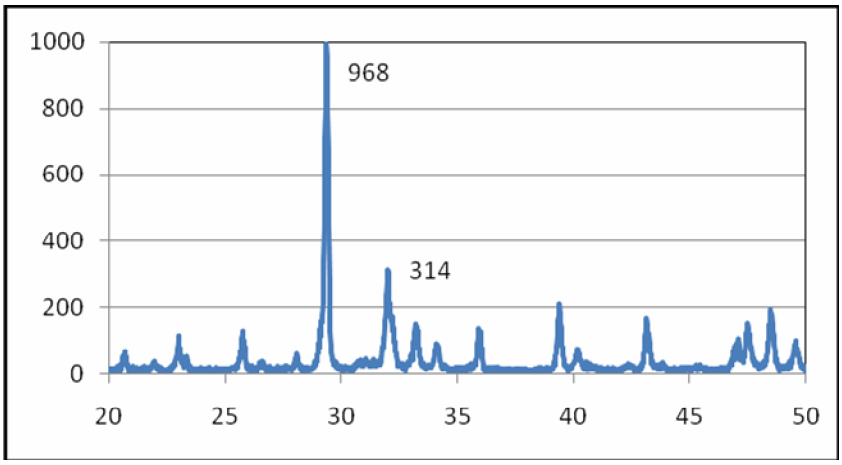

Figure.16 XRD Spectra of beneficiated, Akashat phosphate ore using lactic acid leaching

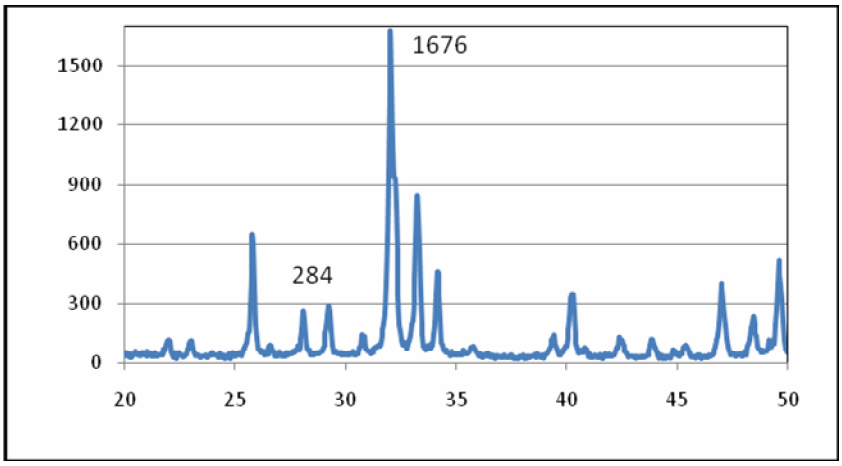

Figure.17 Relation between the three types of analysis FTIR, XRD and LOI

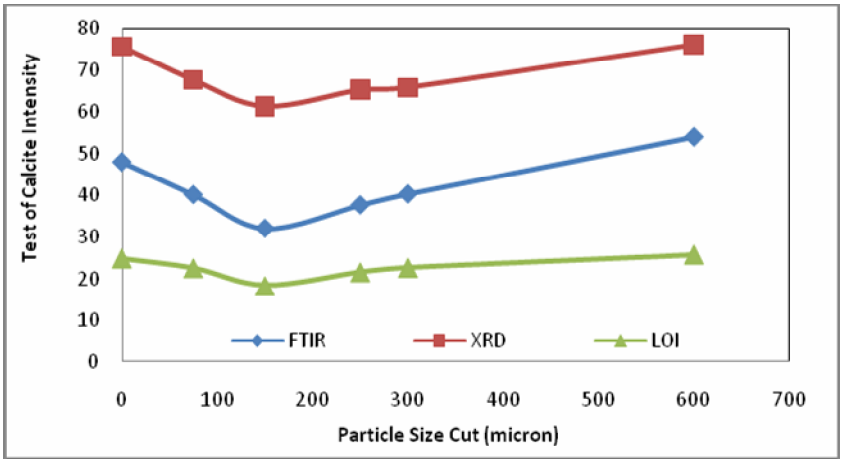

Figure.18 Calibration graph of calcite content based on XRD and FTIR Spectra

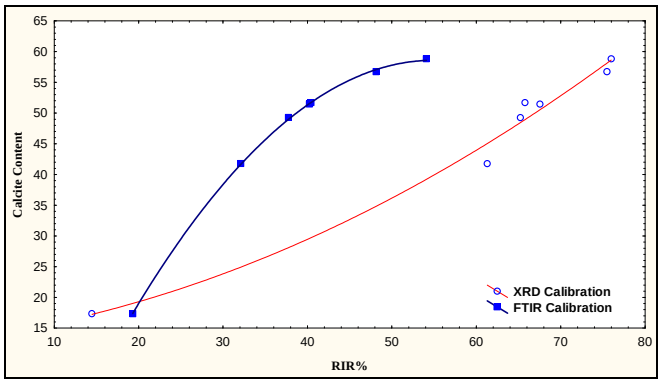

References

Abouzeid, A.Z.M. 2008. Physical and thermal treatment of phosphate ores-An overview. *Int. J. Miner. Process*, 85: 59–84.

Al-Fariss, T.F., Ozbelge, H.O., El-Shall, H.S. 1992. On the phosphate rock beneficiation for the production of phosphoric acid in Saudi Arabia. *J. King Saud Univ. Eng. Sci.*, 4(l): 13–32.

Becker, P. 1983. Phosphates and phosphoric acid, fertilizer science and technology series, Vol. 3. Marcel Dekker Inc., New York.

Bergslien, E.T., Mary Bush, Peter J. Bush. 2008. Identification of cremais using X-ray diffraction spectroscopy and a comparison to trace element analysis. *Forensic Sci. Int.*, 175: 218–226.

Cicil, K., Basma, H., Abdulmajeed, A., Eisa, M.Y. 2013, Beneficiation of Iraqi Akashat phosphate ore using organic acid leaching. *Al-Khwarizmi Eng. J.*, 9(4): 24–38.

Clearfie, A., Reibenspies J., Bhuvanesh, N. 2008. Principles and applications of powder diffraction. Wiley, NY.

Dinnebier, R.E., Simon, J., Billinge, L.

2008. Powder diffraction: theory and practice. RSCX Publishing, Cambridge, UK.

Elliott, J.C. 1994. Structure and chemistry of the apatites and other calcium orthophosphates, Elsevier, Amsterdam.

Featherstone, J.D.B., Pearson, S., LeGeros, R.Z. 1984. An infrared method for quantification of carbonate in carbonated apatites. *Caries Res.,* 18: 63–66.

Gremillion, L.R., McClellan, G.H. 1975. Transactions of society of mining engineers of AIME. *Transactions,* 270.

Griffiths, P.R. 1986. Fourier transform infrared spectrophotometry, 2nd edn. Wiley-Interscience, London. 672 Pp.

Guimarães, R.C., Araujo, A.C., Peres, A.E.C. 2005. Reagents in igneous phosphate ores flotation. *Minerals Eng.,* 18: 199–204.

Herbert T.D., Tom B.A., Burnett C. 1992. Precise major component determination in deep-sea sediments using Fourier transform infrared spectroscopy. *Geochim. Cosmochim. Acta.,* 56: 1759–1763.

Jenkins, R., Snyder, R.L. 1996. Introduction to X-ray powder diffractometry. John Wiley & Sons, New York.

Kirk-Othmer, 1998. Encyclopedia of chemical technology, Vol. 18, 4th edn. John Wiley & Sons Inc., 323 Pp.

Markovic, M., Fowler, B.O., Tung, J. 2004. Preparation and comprehensive characterization ofa calcium hydroxyapatite reference material. *Res. Natl. Inst. Stand. Technol.,* 109: 553–568.

Pecharsky, V.K., Zavalij, P.Y. 2009. Fundamentals of powder diffraction and structural characterization of materials, 2nd edn. Springer, New York.

Ratner, B., Hoffman, A., Schoen, F., *et al.* 2004. Biomaterials science. An introduction to materials in medicine, 2nd edn. Academic Press, London. 851 Pp.

Raynaud S., Champion E., Bernache D., Laval J.P. 2001. Determination of calcium/phosphorus atomic ratio of calcium phosphate apatites using X-ray diffractometry, *J. Am. Ceramic Soc.,* 84: 359–366.

Rungsarit, K., Cherdsak, S., Sakdiphon, T., Sittiporn, P. 2012. Synthesis control and characterization of hydroxyapatite ceramic using a solid state reaction, 1st Mae Fah Luang University International Conference, Thailand, 2012, pp 3–9.

Shirqi, I.S., Tawfiq, O.A. 2010. Akashat phosphate mine, report of the Ministry of Industry and Minerals, Iraqi State Company for Phosphate, Feb. 2010.

Smith, B.C. 1995. Fundamentals of Fourier Transform Infrared Spectroscopy, CRC Press, Boca Raton, FL. 224 Pp.

Tas, C.A. 2007. Porous, biphasic CaCO3-calcium phosphate biomedical cement scaffolds from calcite ($CaCO_3$) powder, *Int. J. Appl. Ceram. Technol.,* 4(2): 152–163.

Van Der Sluis, S. 1987. A clean technology phosphoric acid process, Ph.D. Thesis, Delft University Press, Netherlands.